Biophysical Chemistry 159 (2011) 303–310

Contents lists available at SciVerse ScienceDirect

Biophysical Chemistry

journal homepage: http://www.elsevier.com/locate/biophyschem

Fluorescence correlation spectroscopic examination of insulin and insulin-like growth factor 1 binding to live cells

Peter W. Winter [a], Jeffrey T. McPhee [b], Alan K. Van Orden [b], Deborah A. Roess [a,c], B. George Barisas [a,b,*]

[a] Cell and Molecular Biology Program, Colorado State University, Fort Collins, Colorado 80523, United States
[b] Department of Chemistry, Colorado State University, Fort Collins, Colorado 80523, United States
[c] Department of Biomedical Sciences Colorado State University, Fort Collins, Colorado 80523, United States

HIGHLIGHTS

- FCS permits examination of interactions between biological molecules on individual live cells.
- 2H3-RBL cells express IR and IGF1R homodimers, as well as hybrid IR-IGF1R heterodimers.
- Insulin and IGF1 compete with differing affinities for available binding sites on these cells.
- Hybrid IR-IGF1R heterodimer formation is likely due to random-association of IR and IGF1R monomers.

GRAPHICAL ABSTRACT

Fluorescence correlation spectroscopy reveals details of ligand binding to insulin receptors and IGF1 receptors on single cells. (A) Equilibrium binding of FITC-insulin to the surface of live cells demonstrates two distinct classes of ligand binding sites. (B) Complete dissociation of FITC-insulin from ligand binding sites on live cells occurs over approximately two hours.

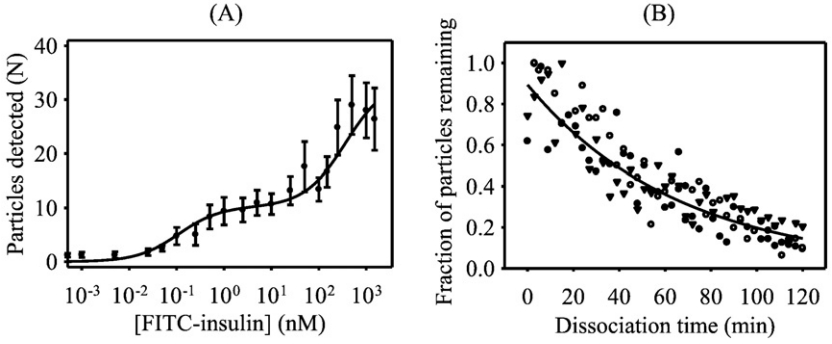

ARTICLE INFO

Article history:
Received 20 July 2011
Received in revised form 10 August 2011
Accepted 11 August 2011
Available online 23 August 2011

Keywords:
Fluorescence correlation spectroscopy
Insulin
IGF1
Receptor surface density
Ligand binding kinetics

ABSTRACT

We used fluorescence correlation spectroscopy to examine the binding of insulin, insulin-like growth factor 1 (IGF1) and anti-receptor antibodies to insulin receptors (IR) and IGF1 receptors (IGF1R) on individual 2H3 rat basophilic leukemia cells. Experiments revealed two distinct classes of insulin binding sites with K_D of 0.11 nM and 75 nM, respectively. IGF1 competes with insulin for a portion of the low-affinity insulin binding sites with K_D of 0.14 nM and for the high-affinity insulin binding sites with K_D of 10 nM. Dissociation rate constants of insulin and IGF1 were determined to be 0.015 min^{-1} and 0.013 min^{-1}, respectively, allowing estimation of ligand association rate constants. Combined, our results suggest that, in addition to IR and IGF1R homodimers, substantial numbers of hybrid IR-IGF1R heterodimers are present on the surface of these cells.

1. Introduction

Traditional approaches to the examination of cell surface receptor density and ligand binding often rely on radio-labeled ligands or fluorescence intensity measurements on bulk solutions [1,2]. Unfortunately, these methods suffer from inherent drawbacks such as the need for

* Corresponding author at: Department of Chemistry, Campus Mail 1872, Colorado State University, Fort Collins, CO 80523, United States. Tel: +1 970 491 6641; fax: +1 970 491 1801.
E-mail address: barisas@lamar.colostate.edu (B.G. Barisas).

0301-4622/$ – see front matter © 2011 Elsevier B.V. All rights reserved.
doi:10.1016/j.bpc.2011.08.003

large numbers of cells and, in cases where receptor numbers are very low, can fail to detect specific binding. In contrast, fluorescence correlation spectroscopy (FCS) is a versatile technique capable of examining interactions between small numbers of biological molecules under physiological conditions [3,4]. Initially introduced in the 1970's [5–7], FCS has since become a versatile tool for the characterization of dynamic biological processes [8,9]. FCS extracts information from the fluctuations in fluorescence intensity that occur as molecules move into and out of a femtoliter-size observation volume [10]. This optically-defined interrogation volume, coupled with high photon sensitivity, permits the examination of as few as 1–2 fluorescing molecules at specific points of interest on the cell membrane or within the cell interior [11,12], allowing real-time measurement of interactions between receptors and ligands [13]. Variations of FCS have recently been used in live cells to examine epidermal growth factor receptor clustering [14], the kinetics of RhoGTPase-Cdc42 effector complex dissociation [15] and interactions between Src peptides and DNA [16]. Ease of use with live cells, the ability to monitor molecular dynamics across a broad timescale and the relatively short time needed for data acquisition make FCS particularly well suited for the examination of molecular interactions at the single molecule level. We report here the use of FCS to determine the surface densities and ligand binding thermodynamics and kinetics of insulin receptors (IR) and insulin-like growth factor 1 receptors (IGF1R) on live 2H3 rat basophilic leukemia (2H3-RBL) cells.

IR and IGF1R are two structurally similar tyrosine kinase receptors with differential effects on cell growth and energy metabolism [17–19]. Because of their physiological importance [20], considerable work has focused on understanding the subtle differences between the two receptors, their ligands and signaling networks [21]. In solution, each receptor is capable of binding both insulin and insulin-like growth factor 1 (IGF1) with nM affinity [20,22,23]. Also, due to random receptor-dimer assembly in the endoplasmic reticulum, a significant fraction of native receptors in some cell types appear to be IR-IGF1R hybrids [24–27], further complicating the analysis of insulin and IGF1 binding kinetics. However, despite considerable literature describing IR, IGF1R and IR-IGF1R hybrid signaling *in vitro*, details of insulin and IGF1 binding to receptors in live cells at the single-molecule level remain elusive.

Our results demonstrate that 2H3-RBL cells express substantial levels of both IR and IGF1R. We also show that insulin and IGF1 each bind to two distinct classes of sites on these cells and that both insulin and IGF1 compete with differing affinities for these binding sites. Finally, we demonstrate that dissociation of FITC-insulin from receptors is sensitive to the concentration of excess insulin available in solution, but is not sensitive to the initial FITC-insulin labeling concentration. Taken together, our results suggest that, in addition to IR and IGF1R homodimers, hybrid IR-IGF1R heterodimers are present on the surface of 2H3-RBL cells and that a significant portion of insulin and IGF1 binding to these cells involves non-cognate receptors and IR-IGF1R hybrids.

2. Experimental procedures

2.1. Materials

2H3-RBL cells were purchased from ATCC (Manassas, VA). Human-recombinant-insulin monovalently-labeled at the *N*-terminus with fluorescein isothiocynate (FITC-insulin) and human-recombinant-IGF1 were purchased from Invitrogen (Carlsbad, CA). Insulin, bovine serum albumin (BSA), biotinylated anti-rabbit secondary antibody and FITC-avidin were purchased from Sigma (St. Louis, MO). Anti-IRα, anti-IGF1Rα and biotinylated anti-IRβ antibodies were purchased from Santa Cruz Biotech (Santa Cruz, CA). Anti-Type I IgE receptor (FcεRI) antibody, FcεRIα was purchased from Upstate Cell Signaling Solutions (Billerica, MA). Rhodamine 6G (R6G) was purchased from Allied Chemical (Vadodara, Gujarat, India). Minimal essential medium (MEM) was purchased from Cellgro (Manassas, VA). Fetal bovine serum (FBS), penicillin G, streptomycin and Fungizone were purchased from Gemini (Sacramento, CA).

2.2. Preparation of cell samples

2H3-RBL cells were maintained in plastic tissue culture dishes in MEM supplemented with 10% FBS, 200 mM L-glutamine, 10,000 U/mL penicillin G, 10 μg/mL streptomycin and 25 μg/mL Fungizone. 24–36 h before experiments cells were seeded onto sterile #1.5 glass-bottom culture dishes, grown to approximately 50% confluence and, unless otherwise indicated, incubated in medium without FBS for at least 12 h before use. All cell labeling protocols were performed in phosphate-buffered saline pH 7.4 (PBS) containing 0.1% BSA (PBS-BSA), except as indicated. All washes were in 1 mL of PBS-BSA buffer for 30 s. Before use, all antibodies, peptides and fluorescent probes were spun for 10 min at maximum speed in a tabletop microcentrifuge to remove aggregates. Cell samples were immersed in 400 μL of buffer during FCS data acquisition, except as noted. All cell labeling and data acquisition were conducted at room temperature.

2.3. Antibody labeling of receptors

To label FcεRI, cells were incubated for 30 min with rabbit-derived primary antibody and washed 4 times. Cells were then incubated for 15 min in 500 nM biotinylated anti-rabbit secondary antibody again followed by 4 washes. Finally, cells were incubated in 250 nM FITC-avidin for 15 min, followed by 4 washes. To label the insulin receptor α-subunit (IRα), cells were serum starved or treated with 10 μM insulin for 1 h or 10% FBS in MEM for 1 h and then incubated for 30 min with rabbit-derived primary antibody and washed 4 times. Cells were then incubated for 15 min in 500 nM biotin conjugated anti-rabbit secondary antibody again followed by 4 washes. Finally, cells were incubated in 250 nM FITC-avidin for 15 min, followed by 4 washes. To label the insulin receptor β-subunit (IRβ), cells were incubated for 30 min with biotinylated primary antibody followed by 4 washes and then incubated for 15 min in 250 nM FITC-avidin, followed by 4 washes. To label IGF1R, cells were incubated for 30 min with rabbit-derived primary antibody specific against the α-subunit of IGF1R (IGF1Rα) and washed 4 times. Cells were then incubated for 15 min in 500 nM biotinylated anti-rabbit secondary antibody again followed by 4 washes. Cells were then incubated in 250 nM FITC-avidin for 15 min, followed by 4 washes.

2.4. Hormone labeling of receptors

In FITC-insulin equilibrium binding experiments, cells were incubated in the indicated concentration of FITC-insulin for 30 min, followed by 4 washes. For insulin and IGF1 competition binding experiments, cells were simultaneously incubated in buffer solutions containing the indicated concentration of FITC-insulin and increasing amounts of either insulin or IGF1for 30 min, and then washed 4 times. In experiments using cells pre-incubated with IGF1, cells were first incubated in the indicated concentration of IGF1 for 30 min and then in a combination of both the indicated amount of IGF1 and 250 nM FITC-insulin for 30 min, followed by 4 washes. To measure FITC-insulin dissociation, cells were labeled with the indicated amount of FITC-insulin for 30 min, washed 4 times and then examined at the times indicated. Alternatively, to investigate the effects of aqueous insulin on FITC-insulin dissociation, cells were labeled with 250 nM FITC-insulin for 30 min, washed 3 times for 30 s in 1 mL of buffer and then incubated in the indicated concentration of insulin for 30 min and washed 3 times. To measure IGF1 dissociation, cells were labeled with 10 nM IGF1 for 30 min, washed 4 times and then incubated in buffer for the indicated time. This was followed by labeling with 250 nM FITC-insulin for 30 min and 4 washes.

2.5. FCS instrumentation

FCS experiments were performed using a modified Nikon TE1000 inverted microscope equipped with a 100×, 1.25 NA oil-immersion objective, an Omnichrome Melles-Griot multi-line air-cooled argon ion laser, two Perkin Elmer single photon counting modules (SPCM-AQR-14) and an ALV-6010 digital hardware correlator. This apparatus has been described in detail previously [28]. Based on FCS measurements of aqueous R6G diffusion, the $1/e^2$ radius r_o of the laser excitation beam at the sample in our system was determined to be 241 nm (data not shown). To obtain the greatest signal-to-noise ratio while minimizing the effects of probe photobleaching on receptor density estimates and ligand binding kinetics, the intensity of the laser excitation beam at the sample was attenuated to <100 μW using neutral density filters [29]. The laser excitation beam was focused on the apical cell membrane by adjusting the objective z-position to maximize detector count rates and minimize diffusional correlation times (τ_D) as described by Ries and Schwille [12]. Relevant portions of individual FCS traces were analyzed by weighted least-squares fitting of $g(\tau)$ to Eq. (3) to obtain estimates of the effective number of particles detected (N) and the diffusional correlation time (τ_D) for both receptor-bound and aqueous particles.

2.6. Analysis of fluorescence intensity fluctuations

All FCS data were analyzed using methods similar to those previously described by Schwille et al. [3], where the normalized intensity fluctuation autocorrelation function is defined as

$$g(\tau) = \langle \delta F(t) \delta F(t+\tau) \rangle / \langle F(t) \rangle 2 \tag{1}$$

where $F(t)$ is the mean fluorescence intensity at time t and

$$\delta F(t) \equiv F(t) - \langle F(t) \rangle \tag{2}$$

is the corresponding fluorescence intensity fluctuation about the mean.

Given a Gaussian excitation spot of $1/e^2$ radius r_o and a substance with diffusion constant D, the autocorrelation function describing two-dimensional diffusion within the cell membrane is

$$g(\tau) = \frac{1}{N}\left(\frac{1}{1+\tau/\tau_d}\right) \tag{3}$$

where N is the effective number of correlating particles detected in the illumination zone and

$$\tau_d = \frac{r_0^2}{4D} \tag{4}$$

is the characteristic time of correlation decay.

2.7. Analysis of ligand–receptor interactions on live cells

Analysis of FCS data showed that the number N of membrane bound particles detected depended on the concentration of receptor-specific fluorophore and competing ligands. To evaluate the specific binding capacity and equilibrium dissociation constant K_D of each fluorophore-conjugated ligand for receptors, data were fit to hyperbolic functions describing either one or two-site sequential binding.

$$N = \frac{cN_1}{K_{D1}+c} + \frac{cN_2}{K_{D2}+c} \tag{5}$$

where N is the number of particles detected, c is the concentration of fluorophore-conjugated receptor-specific probe and N_1, N_2 are the maximum numbers of bound particles detected at saturating concentration of receptor-specific probe, exhibiting dissociation constants K_{D1} and K_{D2}, respectively. For single-site binding, N_2 is fixed at zero.

The density σ of receptors on the surface of live cells was calculated as

$$\sigma = \frac{N_1 + N_2}{\pi {r_o}^2}. \tag{6}$$

When analyzing the competitive binding between two ligands, the concentration $[I]_{1/2}$ of the competing ligand which gave 50% inhibition of probe binding was determined using

$$N = N_o + \frac{N_{max} - N_o}{1 + [I]/[I]_{1/2}} \tag{7}$$

where N_{max} and N_o are the numbers of detected particles at the indicated concentration [L] of fluorophore-conjugated ligand as observed at zero and maximum concentrations of competing ligand, respectively.

From $[I]_{1/2}$ the effective dissociation constant K_I can be calculated according to the method of Cheng et Prusoff [30] as

$$K_I = \frac{[I]_{1/2}}{1 + {}^{[L]}/_{K_D}} \tag{8}$$

In ligand-dissociation experiments for both FITC-insulin and IGF1, data were fit to a single component exponential decay function

$$N = N_o + (N_{max} - N_o) e^{-tk_{off}} \tag{9}$$

where t is time and k_{off} is the dissociation rate constant.

2.8. Presentation of results

Each data point shown in figures represents the results of FCS measurements on 14–20 individual 2H3-RBL cells from at least two separate experiments. Values presented in figures, text and tables, excluding Figs. 4 and 5a, are the arithmetic mean ± SD. To improve visual clarity, Figs. 4 and 5a show the mean ± SEM.

3. Results

3.1. Binding of fluorescent probes to live cells

We used FCS to analyze the dynamics of peptide-conjugated fluorescent probes in solution and when bound to receptors on the membranes of live 2H3-RBL cells. τ_D values for these probes in solution correspond to lateral diffusion constants of approximately 5×10^{-7} cm^2 s^{-1} as is appropriate for small proteins in solution (Fig. 1). When bound to receptors on live 2H3-RBL cells the fluorescence emission of the FITC-conjugated receptor-specific probes was localized to the cell-surface and detected particles exhibited τ_D that correspond to lateral diffusion constants of between 10^{-9} cm^2 s^{-1} and 10^{-10} cm^2 s^{-1} as is appropriate for cell-surface receptors (Fig. 1). Receptors on live cells labeled with either FITC-insulin or a sandwich of IR-specific antibody, biotinylated-secondary antibody and FITC-avidin had similar diffusion times while antibody-labeled Fcε receptors exhibited somewhat slower diffusion. After an initial (~10 s) illumination phase to deplete immobile particles [3,31], the photon count rates from both avalanche photodiodes during live cell labeling experiments were steady, indicating that there was no appreciable photobleaching of FITC-insulin over the time-scale of these experiments (data not shown).

To test the specificity of our probes, we performed FCS measurements on cells incubated with FITC-avidin while omitting either primary or secondary antibody or both. No appreciable surface-localized fluorescence was observed under these conditions (data not shown).

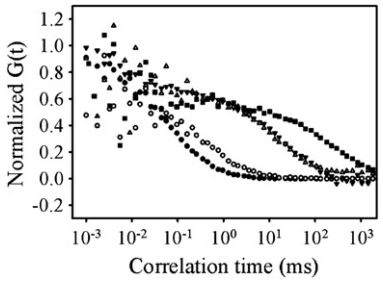

Fig. 1. Normalized autocorrelation functions for fluorescent probes in solution and bound to receptors on the surface of live 2H3-RBL cells. [●] FITC-insulin (aqueous), [○] FITC-avidin (aqueous), [Δ] FITC-insulin (live cells), [▼] FITC-avidin (bound to IR specific antibody on live cells), [■] FITC-avidin (bound to FcεRI specific antibody on live cells). To improve clarity not all time points are shown.

3.2. Determination of FcεRI, IR and IGF1R cell-surface densities

2H3-RBL cells are known to express both FcεRI [32] and IR [33]. Fig. 2a shows correlation data obtained from live 2H3-RBL cells labeled with increasing concentrations of primary antibody specific for an external epitope of FcεRI. Non-linear least-squares analysis of these data using a single-site binding model showed that the FcεRI-specific antibody binds to an estimated 540 receptors μm^{-2} with K_D of 61 nM (Table 1). A total of 170,000 FcεRI per cell was calculated from the receptor surface density assuming 2H3-RBL cells each have an average surface area of 314 μm^2 [32]. This is consistent with previous estimates of between 200,000 and 300,000 receptors per cell for this cell type [32,34–37].

Two different primary antibodies specific for external epitopes of either IRα or IRβ, respectively, were then used to determine the density of IR on the surface of live 2H3-RBL cells. Measurements made with both primary antibodies resulted in similar estimates of IR surface density (Fig. 2b and c). Use of the IRα-specific antibody yielded 190 receptors μm^{-2} or 60,000 per cell, while the IRβ-specific antibody yielded 196 receptors μm^{-2} or 62,000 per cell (Table 1). However, despite providing similar estimates of IR density, the two IR-specific antibodies exhibited distinct K_D. The IRα-specific antibody appeared to bind receptors with K_D of 23 nM, while the IRβ-specific antibody appeared to bind with K_D of 163 nM (Table 1).

We also estimated the density of IGF1R on these cells using an antibody specific for IGF1Rα. This antibody appeared to bind 161 receptors μm^{-2} or 51,000 per cell with a K_D of 2 nM (Fig. 2d and Table 1).

3.3. Equilibrium binding of FITC-insulin to live cells

To evaluate the binding of insulin to IR on live cells, we used a commercially-available *N*-terminally labeled FITC-insulin. In contrast to the binding of receptor-specific antibodies, equilibrium binding of FITC-insulin appeared to be fit best by a two-site sequential model (Fig. 3a). Scatchard analysis of FITC-insulin binding also showed a curvilinear 'concave up' pattern indicating two classes of FITC-insulin binding sites (Fig. 3b). Using least-squares analysis, we determined the K_D of the two classes of FITC-insulin binding sites to be 0.11 nM and 75 nM with surface densities of 49 sites μm^{-2} and 124 sites μm^{-2}, respectively (Table 2). The total number of FITC-insulin binding sites identified in these experiments was approximately 54,000 per cell.

FITC-insulin binding to receptors on 2H3-RBL cells was almost completely blocked by pre-incubating cells in medium containing 10% FBS or 10 μM insulin (Table 3), treatments which had no effect on the binding of the IRα antibody (Fig. 2b). Binding of 250 nM FITC-insulin was also partially blocked by pre-incubation of cells with between 0.1 and 10 nM IGF1 (Table 3). The diminished binding of FITC-insulin to cells that have been pre-incubated with increasing concentrations of IGF1 is assumed to result from occupancy of the FITC-insulin binding sites by IGF1. This suggests that at least 67 ± 28 μm^{-2} of the low affinity FITC-insulin binding sites, approximately $21{,}000 \pm 9000$ per cell, are able to bind IGF1 with K_D of 0.14 ± 0.04 nM (Fig. 4).

3.4. Insulin and IGF1 competitive binding to live cells

When cells are labeled simultaneously with FITC-insulin and either insulin or IGF1, equilibrium competition for available binding sites is

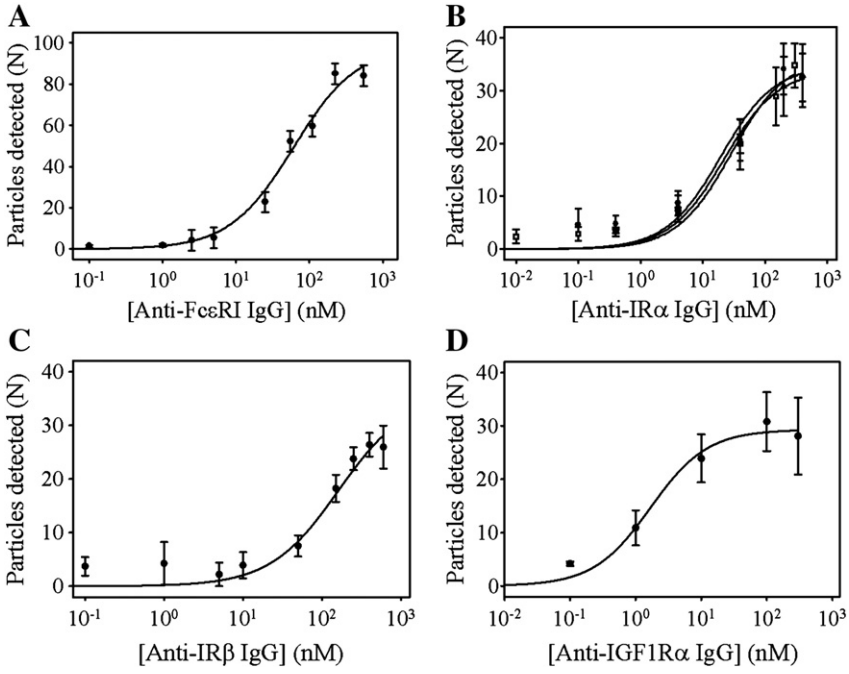

Fig. 2. Equilibrium binding of receptor specific antibodies to live 2H3-RBL cells. Binding of FITC-avidin to cells labeled with increasing concentrations of, A) [●] FcεRI specific antibody, B) [●] IRα-specific antibody, also shows that pre-incubation of the cells with [▲] 10 μM insulin or medium containing [□] 10% FBS has no effect on antibody labeling of IR, C) [●] biotinylated IRβ-specific antibody, or D) [●] IGF1Rα-specific antibody.

Table 1
Surface density of IR, IGF1R and FcεRI on 2H3-RBL cells and binding parameters of the primary antibody used to identify each receptor.

Receptor	Antibody	N[a]	σ (receptors μm^{-2})	Total receptors[b]	KD (nM)[c]
IR	IRα	34.6 ± 1.2	190 ± 7	60,000 ± 2000	23 ± 4
IR	IRβ	35.8 ± 4.5	196 ± 25	62,000 ± 8000	163 ± 56
IGF1R	IGF1Rα	29.3 ± 1.2	161 ± 7	51,000 ± 2000	2 ± 1
FcεRI	FcεRIα	98.4 ± 19.6	540 ± 108	170,000 ± 34,000	61 ± 23

[a] N is the effective number of particles detected in the FCS laser-spot at saturating concentrations of primary receptor-specific antibody.
[b] Value for total receptors per cell assumes the surface area of a 2H3-RBL cell is 314 μm^{-2} [32].
[c] Values presented for K_D reflect the binding of primary antibody to specific receptors on live 2H3-RBL cells.

observed (Fig. 5a and b). In such competition binding experiments using a probe concentration of 0.1 nM FITC-insulin, insulin competed with K_I of 0.09 nM (Table 4). However, the apparent K_I of insulin for FITC-insulin binding sites increased when probed with increasing concentrations of FITC-insulin. In addition, IGF1 also competed with 0.1 nM FITC-insulin for binding sites with a K_I of 9.4 nM (Table 5); and, similar to insulin, the apparent K_I of IGF1 for FITC-insulin binding sites also increased when probed with increasing concentrations of FITC-insulin.

3.5. Dissociation rates of FITC-insulin and IGF1 from live cells

The dissociation of FITC-insulin from the surface of 2H3-RBL cells in the absence of excess solution phase insulin was monitored by measuring the number of particles remaining bound to cells every 3 min for 2 h. Fig. 6a shows that, when incubated in insulin-free PBS-BSA buffer, cells labeled with FITC-insulin concentrations ranging from 1 to 100 nM behaved similarly and exhibited k_{off} values between 0.014 min^{-1} and 0.017 min^{-1} (Table 6).

However, dissociation of FITC-insulin was sensitive to the concentration of excess insulin available in solution. Cells labeled with 250 nM FITC-insulin were incubated for 30 min in the indicated concentrations of excess insulin, then washed and observed (Fig. 6b). It appears that the rate of FITC-insulin dissociation increased in the presence of unlabeled insulin at concentrations below 10^{-8} while, at insulin

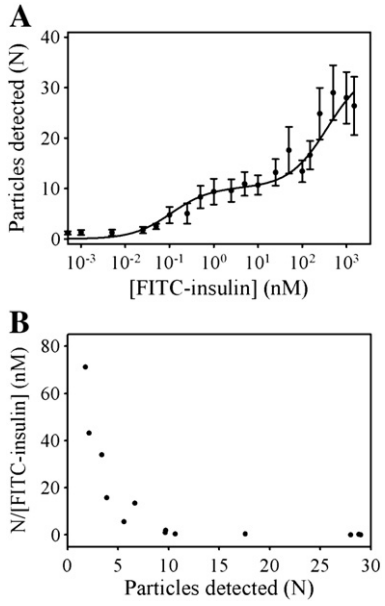

Fig. 3. A) [●] Equilibrium binding of FITC-insulin to receptors on the surface of serum starved 2H3-RBL cells was fit to a two-site sequential model. B) [●] Scatchard analysis of FITC-insulin binding displays a concave-up curvilinear pattern.

Table 2
Equilibrium binding of FITC-insulin to receptors on the surface of live 2H3-RBL cells.

Binding Site	N[a]	σ (receptors μm^{-2})	Total receptors[b]	K_D (nM)[c]
1	9.0 ± 1.1	49 ± 6	15,000 ± 2000	0.11 ± 0.05
2	22.6 ± 1.4	124 ± 8	39,000 ± 3000	75 ± 23

[a] N is the upper limit for detected particles for sites 1 and 2.
[b] Value for total receptors per cell assumes the surface area of a 2H3-RBL cell is 314 μm^{-2} [32].
[c] Values presented for K_D were obtained using a two-site sequential model of ligand-receptor binding.

concentrations greater than 10^{-8} M, the rate of FITC-insulin dissociation decreased.

Dissociation of IGF1 was monitored by examining the partial blocking of FITC-insulin binding at various times after pre-incubating cells with IGF1 (Fig. 6c). Diminished binding of 250 nM FITC-insulin after pre-incubating cells with 10 nM IGF1 is assumed to result from occupancy of FITC-insulin binding sites by IGF1 as was discussed in Section 2.4. Using this method, we estimated that the k_{off} of IGF1 from receptors on live 2H3-RBL cells is 0.013 min^{-1} (Table 6).

3.6. Estimated association rates for insulin and IGF1 binding to live cells

Our results provide experimentally-determined values for either K_D or K_I, and k_{off} for FITC-insulin or insulin and IGF1 reversibly binding to receptors on 2H3-RBL cells. From these data we estimated the rate of association k_{on} for each ligand binding to both high and low affinity sites. The k_{on} for high and low affinity FITC-insulin binding sites were estimated to be 1.4×10^8 M^{-1} min^{-1} and 2×10^5 M^{-1} min^{-1}, respectively. Alternatively, the k_{on} of IGF1 to high affinity IGF1 binding sites identified after pre-incubation with IGF1 was estimated to be 7.1×10^9 M^{-1} min^{-1}, while the k_{on} of IGF1 to low-affinity IGF1 binding sites identified in competitive labeling experiments between IGF1 and FITC-insulin was estimated to be 1.4×10^6 M^{-1} min^{-1}.

4. Discussion

The present work emphasizes the utility of FCS for the quantitative examination of membrane receptor ligand binding in living cells at the single molecule level [14,15,34]. Localization of fluorophore-conjugated ligand fluorescence to the cell membrane, specificity of ligand binding, and differences in lateral diffusion between solution-phase and membrane localized fluorophore-conjugated ligands allows specific examination of fluorophore-conjugated ligands bound to membrane receptors even in the presence of solution-phase fluorophore-conjugated ligand [3].

In the present study, use of antibodies specific against either α or β subunits of IR led to initial estimates of between 190 and 196 receptors μm^{-2} or approximately 60,000 receptors per cell. Labeling of receptors with FITC-insulin led to a slightly lower estimate of approximately 54,000 total receptors. This is similar to previous work by Rigler et al. who estimated the density of IR on live

Table 3
Reduced binding of FITC-insulin to receptors on 2H3-RBL cells after pre-incubation with insulin, FBS or IGF1.

Treatment	N[a]	Diff (N)[b]
None	24.8 ± 5.1	NA
Insulin (10μM)	2.0 ± 1.6	22.8 ± 5.1
FBS (10%)	4.6 ± 1.0	20.2 ± 5.1
IGF1 (0.1nM)	19.8 ± 1.6	5.2 ± 5.1
IGF1 (1nM)	14.1 ± 3.1	10.9 ± 5.1
IGF1 (10nM)	12.9 ± 0.8	12.1 ± 5.1

[a] N is the number of particles detected after labeling with 250 nM FITC-insulin.
[b] Estimated as the difference between the number of FITC-insulin bound to untreated cells and to cells with the indicated pre-treatment.

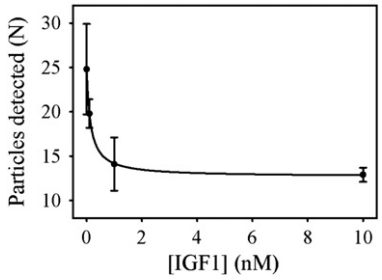

Fig. 4. [●] Indirect observation of IGF1 binding to live 2H3-RBL cells. Pre-incubation with increasing concentrations of IGF1 reduced the apparent binding of 250 nM FITC-insulin to live cells.

human renal cells to be approximately 200 μm^{-2} [38]. Estimation of IGF1R numbers using an IGF1Rα specific antibody also identified 161 receptors μm^{-2} or 51,000 per cell. However, FCS measurements enumerate the total of all diffusing species binding particular fluorescent ligands, hence apparent numbers of IR and IGF1R estimated using anti-IR or anti-IGF1R antibodies, respectively, also include IR/IGF1R hybrids. Thus, it is likely that neither IR nor IGF1R densities are actually this high [27]. We also suggest that similar overestimation of IR and IGF1R occurs when using fluorophore-conjugated peptide ligands such as FITC-insulin, which in addition to binding cognate receptors, also bind with measurable affinity to non-cognate and hybrid IR-IGF1R.

Multiple lines of research have shown that the binding of insulin to IR is negatively cooperative *in vitro* [20,39] with insulin binding to IR at two sites, each with a distinct K_D [40,41]. Similarly, our results show that FITC-insulin binds two classes of sites on 2H3-RBL cells and exhibits an upward curving Scatchard plot. This curvilinear Scatchard plot is commonly seen during examination of insulin binding and was previously observed by Zhong and coworkers when examining rhodamine-labeled insulin (Rh-insulin) binding to human renal cells using FCS [42]. These investigators attributed such curvilinear Scatchard plots either to the negative cooperative binding of insulin to IR or to

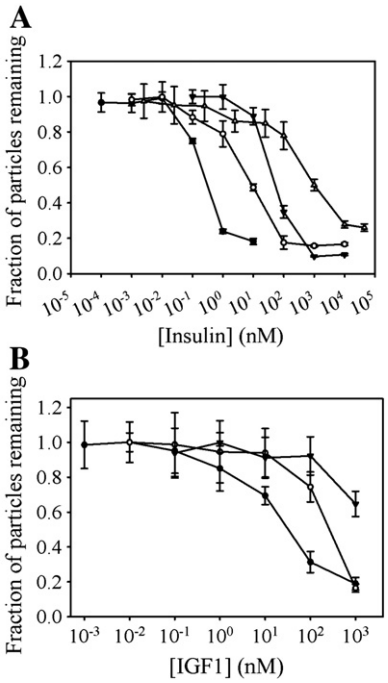

Fig. 5. Competitive binding of insulin and IGF1 to receptors on 2H3-RBL cells. A) Competitive binding of insulin and [●] 0.1 nM, [○] 1 nM, [▼] 10 nM, or [Δ] 50 nM FITC-insulin to receptors on 2H3-RBL cells. B) Competitive binding of IGF1 and [●] 0.1 nM, [○] 1 nM, or [▼] 10 nM FITC-insulin to receptors on 2H3-RBL cells.

Table 4
Competitive binding of insulin and FITC-insulin to receptors on live 2H3-RBL cells.

[FITC-insulin] (nM)	$I_{1/2}$ (nM)[a]	K_I (nM)[b]	N_{max} [c]	N_o[d]
0.1	0.18 ± 0.02	0.09 ± 0.01	5.9 ± 0.1	1.1 ± 0.1
1	5.4 ± 1.6	0.54 ± 0.16	9.1 ± 0.3	1.3 ± 0.3
10	47.4 ± 3.4	0.52 ± 0.04	10.4 ± 0.1	1.0 ± 0.1
50	590 ± 250	1.29 ± 0.55	12.4 ± 0.2	2.1 ± 0.8

[a] $I_{1/2}$ values were obtained by fitting Eq. (7) to binding data for insulin concentrations between 10^{-4} and 10^{5} nM.
[b] Values for K_I were obtained from $I_{1/2}$ using Eq. (8).
[c] N_{max} is the apparent number of particles detected in the absence of competing insulin.
[d] N_o is the apparent number of particles detected at saturating insulin concentrations.

separate classes of receptors with differing affinities for insulin. However, FCS monitors the approximate total number of separately diffusing species and is somewhat insensitive to the absolute brightness of each species (Supplement 1). Once a FITC-insulin or Rh-insulin molecule binds to an individual IR, the binding of subsequent fluorophore-labeled insulin molecules to this IR, despite changing the absolute magnitude of fluorescence fluctuations as the receptor enters and exits the interrogation volume, has only a limited effect on the normalized autocorrelation function [3]. With this in mind, we suggest that the majority of receptors observed in the present work on live 2H3-RBL cells that bind FITC-insulin with low affinity, and those observed by Zhong and coworkers that bind Rh-insulin with low affinity [42], may not be IR but are more likely either IGF1R or IR-IGF1R hybrids.

Negative cooperativity in insulin binding to IR was apparent from our measurements of FITC-insulin dissociation. Our results demonstrate that FITC-insulin dissociation varied with the concentration of excess insulin available in solution. FITC-insulin dissociation initially accelerated with increasing concentrations of excess insulin, but then decreased at insulin concentrations above 10^{-8} M. However, in the absence of excess insulin, the dissociation rate of FITC-insulin was independent of the initial labeling concentration. Acceleration of ligand dissociation in response to excess solution-phase ligand can indicate negatively-cooperative binding and, while not necessarily relevant physiologically, the effects of insulin concentrations above 10^{-8} M provide insight into the mechanism of insulin binding to IR and support the harmonic oscillator model of insulin and IGF1 binding proposed by Kiselyov and coworkers [17].

Our results also demonstrate that FITC-insulin, insulin and IGF1 compete for binding to available receptors on live 2H3-RBL cells. At a FITC-insulin labeling concentration of 0.1 nM, approximately equal to FITC-insulin's high-affinity site K_D, the binding of FITC-insulin and insulin are quite similar, indicating that conjugation of fluorescein to insulin does not affect IR binding, and values of K_I obtained for IGF1 competing with 0.1 nM FITC-insulin agree with existing literature showing that IR can bind IGF1 with nM affinity [20]. At higher levels of receptor occupancy, obtained by increasing the labeling concentration of FITC-insulin, the affinities of insulin and IGF1 relative to FITC-insulin appear to decrease. Of course, for competitive ligand binding to a single site, K_I must be independent of the level of site

Table 5
Competitive binding of IGF1 and FITC-insulin to receptors on live 2H3-RBL cells.

[FITC-insulin] (nM)	$I_{1/2}$ (nM)[a]	K_I (nM)[b]	N_{max}[c]	N_o[d]
0.1	21.1 ± 8.1	9.4 ± 3.6	5.9 ± 0.1	0.7 ± 0.4
1	143.7 ± 72.4	10.9 ± 5.5	9.6 ± 0.2	0.5 ± 0.1
10	1727.6 ± N.A.	14.5 ± N.A.	10.7 ± 0.5	1 ± N.A.

[a] $I_{1/2}$ values were obtained by fitting Eq. (7) to binding data for IGF1 concentrations between 10^{-3} and 10^{3} nM.
[b] Values for K_I were obtained from $I_{1/2}$ using Eq. (8).
[c] N_{max} is the apparent number of particles detected in the absence of competing IGF1.
[d] N_o is the apparent number of particles detected at saturating IGF1 concentrations.

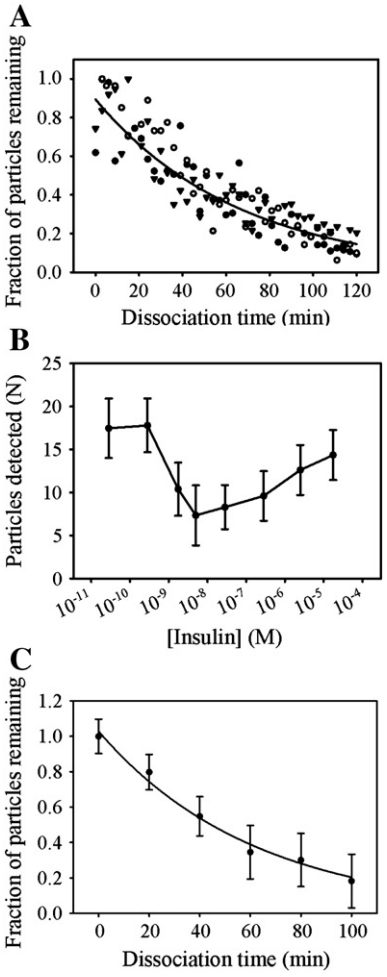

Fig. 6. Dissociation of insulin and IGF1 from receptors on 2H3-RBL cells. A) Dissociation of [●] 1 nM, [○] 10 nM, or [▼] 100 nM FITC-insulin from receptors on live 2H3-RBL cells in the absence of excess aqueous insulin. For each condition, every data point shown is from a different cell. B) [●] Effects of excess aqueous insulin on the dissociation of FITC-insulin from live 2H3-RBL cells. The k_{off} of FITC-insulin initially increases with increasing insulin concentrations but then, at concentrations of insulin $>10^{-8}$ nM, decreases. C) [●] The dissociation of 10 nM IGF1 is shown. Data points represent the reduction in the binding of 250 nM FITC-insulin compared to cells not pre-incubated with IGF1.

occupancy. However, the present system exhibits multiple binding affinities and/or negative cooperativity as ligands bind multivalently to a mixture of IR, IGF1R and IR-IGF1R hybrids. In such a system, increasing receptor occupancy reflects the involvement of progressively lower affinity FITC-insulin binding sites. Hence the apparent dissociation constants K_I of competing ligands will increase.

Like IR, IGF1R exhibits complex ligand binding kinetics [43,44], binding its cognate ligand IGF1 strongly, but also binding insulin with nM affinity [20]. Additionally, evidence suggests that IR-IGF1R hybrids, much like IGF1R, bind IGF1 strongly, but can also bind insulin with nM affinity [45–48]. We found that 67 sites μm^{-2} of the 124 sites μm^{-2} that bind insulin with low affinity also bind IGF1 with high affinity. This suggests that these receptors are likely not IR, but rather are either IGF1R or IR-IGF1R hybrids. However, the total number of receptors identified using FITC-insulin on 2H3-RBL cells was only slightly more than half the combined number of receptors identified using IR- and IGF1R-specific antibodies, suggesting that a substantial portion of these receptors are in fact IR-IGF1R hybrids.

Table 6
Rate of FITC-insulin and IGF1 dissociation from receptors on 2H3-RBL cells.

Ligand	Concentration (nM)	k_{off} (min^{-1})	$t_{1/2}$ (min)[a]
FITC-insulin	1	0.014 ± 0.001	50 ± 4
FITC-insulin	10	0.017 ± 0.001	41 ± 4
FITC-insulin	100	0.015 ± 0.001	46 ± 4
IGF1	10	0.013 ± 0.004	52 ± 16

[a] Value for $t_{1/2}$ determined using the approximation $t_{1/2} = 0.69/k_{off}$.

The current model describing the formation of IR and IGF1R homodimers and IR-IGF1R hybrids assumes that IR and IGF1R monomers randomly associate to form dimers within the endoplasmic reticulum [27]. This model allows calculation of relative amounts of IR homodimers, IR-IGF1R hybrids and IGF1R homodimers from the ratio of IGF1R monomers to IR monomers (Supplement 2). If the results of receptor-specific antibody experiments are used as a first approximation of the ratio of IGF1R monomers to IR monomers on these cells, this model predicts about 30% and 20% of cell surface species are IR and IGF1R-homodimers, respectively, while IR-IGF1R hybrids account for fully 50% of total cell surface receptors. Since receptor-specific labeling indicated the surface density of IR monomer-containing species is 190 μm^{-2}, this suggests that only 57 μm^{-2} of these species are actual IR homodimers, which is similar to the 49 μm^{-2} of species on these cells that bind FITC-insulin with high affinity. This model also predicts an IGF1R homodimer density of approximately 38 μm^{-2}. Given the known similarity between the K_D's of IGF1R and IR-IGF1R hybrids for IGF1, we would anticipate that the 161 species μm^{-2} identified with IGF1R-specific antibody should bind IGF1 with high affinity. However, we identified only 67 species μm^{-2} binding IGF1 with high affinity, a discrepancy which is likely the result of our inability to observe IGF1 binding directly. Taken together, our results are generally consistent with random association of IR and IGF1R monomers in the endoplasmic reticulum and suggest that IR-IGF1R hybrids represent a major receptor species on the surface of 2H3-RBL cells.

Supplementary materials related to this article can be foundonline at doi:10.1016/j.bpc.2011.08.003.

Acknowledgments

We would like to thank Jonathan Gerding for his assistance with alignment of FCS instrumentation. This project was supported in part by the NSF (CHE0628260, MCB1024688) and by the American Heart Association (AHA0650081Z).

References

[1] B. Goldstein, R.G. Posner, D.C. Torney, J. Erickson, D. Holowka, B. Baird, Competition between solution and cell surface receptors for ligand. Dissociation of hapten bound to surface antibody in the presence of solution antibody, Biophysical Journal 56 (1989) 955–966.
[2] J. Erickson, B. Goldstein, D. Holowka, B. Baird, The effect of receptor density on the forward rate constant for binding of ligands to cell surface receptors, Biophysical Journal 52 (1987) 657–662.
[3] P. Schwille, U. Haupts, S. Maiti, W.W. Webb, Molecular dynamics in living cells observed by fluorescence correlation spectroscopy with one- and two-photon excitation, Biophysical Journal 77 (1999) 2251–2265.
[4] S.A. Kim, K.G. Heinze, P. Schwille, Fluorescence correlation spectroscopy in living cells, Nature Methods 4 (2007) 963–973.
[5] D.E. Magde, Elliot, Webb, Watt, Thermodynamic fluctuations in a reacting system—measurement by fluorescence correlation spectroscopy, Physical Review Letters 29 (1972) 705–708.
[6] E.L. Elson, D. Magde, Fluorescence correlation spectroscopy. I. conceptual basis and theory, Biopolymers 13 (1974) 1–27.
[7] D. Magde, E.L. Elson, W.W. Webb, Fluorescence correlation spectroscopy. II. An experimental realization, Biopolymers 13 (1974) 29–61.
[8] W. Webb, Commentary on the pleasure of solving impossible problems of experimental physiology, Annual Review of Physiology 68 (2006) 1–28.
[9] H.-T. He, D. Marguet, Detecting nanodomains in living cell membrane by fluorescence correlation spectroscopy, Annual Review of Physical Chemistry 62 (2011) 417–436.
[10] P. Schwille, Cell Biochemistry and Biophysics, vol. 34, Humana Press Inc., 2001, pp. 383–408.
[11] P. Schwille, J. Korlach, W. Webb, Fluorescence correlation spectroscopy with single-molecule sensitivity on cell and model membranes, Cytometry 36 (1999) 176–182.

[12] J. Ries, P. Schwille, New concepts for fluorescence correlation spectroscopy on membranes, Physical Chemistry 10 (2008) 3487–3497.
[13] A. Pramanik, R. Rigler, Ligand-receptor interactions in the membrane of cultured cells monitored by fluorescence correlation spectroscopy, Biological Chemistry 382 (2001) 371–378.
[14] S. Saffarian, U. Li, E. Elson, L. Pike, Oligomerization of the EGF receptor investigated by life cell fluorescence intensity distribution analysis, Biophysical Journal 93 (2007) 1021–1031.
[15] T. Sudhaharan, P. Liu, Y.H. Foo, W. Bu, K.B. Lim, T. Wohland, S. Ahmed, Determination of in vivo dissociation constant, K_D, of Cdc42-effector complexes in live mammalian cells using single wavelength fluorescence cross-correlation spectroscopy, Journal of Biological Chemistry 284 (2009) 13602–13609.
[16] V. Vukojevic, D.K. Papadopoulos, L. Terenius, W.J. Gehring, R. Rigler, Quantitative study of synthetic Hox transcription factor DNA interactions in live cells, Proceedings of the National Academy of Sciences 107 (2010) 4093–4098.
[17] V.V. Kiselyov, S. Versteyhe, L. Gauguin, P. De Meyts, Harmonic oscillator model of the insulin and IGF1 receptors' allosteric binding and activation, Molecular Systems Biology 5 (2009) 243.
[18] L. Gauguin, B. Klaproth, W. Sajid, A.S. Andersen, K.A. McNeil, B.E. Forbes, P. De Meyts, Structural basis for the lower affinity of the insulin-like growth factors for the insulin receptor, Journal of Biological Chemistry 283 (2008) 2604–2613.
[19] J. Dupont, D. LeRoith, Insulin and insulin-like growth factor 1 receptors: similarities and differences in signal transduction, Hormone Research 55 (2001) 22–26.
[20] P. De Meyts, J. Whittaker, Structural biology of insulin and IGF1 receptors: implications for drug design, Nature Reviews Drug Discovery 1 (2002).
[21] C.M. Taniguchi, B. Emanuelli, C.R. Kahn, Critical nodes in signalling pathways: insights into insulin action, Nature Reviews Molecular Cell Biology 7 (2006) 85–96.
[22] M.C. Lawrence, N.M. McKern, C.W. Ward, Insulin receptor structure and its implications for the IGF-1 receptor, Current Opinion in Structural Biology Catalysis and regulation/Proteins 17 (2007) 699–705.
[23] C. Ward, M. Lawrence, V. Streltsov, T. Garrett, N. McKern, M.-Z. Lou, G. Lovrecz, T. Adams, Structural insights into ligand-induced activation of the insulin receptor, Acta Physiologica 192 (2008) 3–9.
[24] H. Zhang, A. Pelzer, D. Kiang, D. Yee, Down-regulation of Type 1 insulin-like growth factor receptor increases sensitivity of breast cancer cells to insulin, Cancer Research 67 (2007) 391–397.
[25] G. Pandini, R. Vigneri, A. Costantino, F. Frasca, A. Ippolito, Y. Fujita-Yamaguchi, K. Siddle, A. Goldfine, A. Belfiore, Insulin and insulin-like growth factor-1 (IGF-1) receptor overexpression in breast cancer leads to insulin/IGF-1 hybrid receptor overexpression: evidence for a second mechanism of IGF-1 signaling, Clinical Cancer Research 5 (1999) 1935–1944.
[26] A.M. Rowzee, D.L. Ludwig, T.L. Wood, Insulin-like growth factor type 1 receptor and insulin receptor isoform expression and signaling in mammary epithelial cells, Endocrinology 150 (2009) 3611–3619.
[27] E. Bailyes, B. Nave, M. Soos, S. Orr, A. Hayward, K. Siddle, Insulin receptor/IGF-1 receptor hybrids are widely distributed in mammalian tissues: quantification of individual receptor species by selective immunoprecipitation and immunoblotting, Biochemical Journal 327 (1997) 209–215.
[28] K. Fogarty, J. McPhee, E. Scott, A. Van Orden, Probing the ionic atmosphere of single-stranded DNA using continuous flow capillary electrophoresis and fluorescence correlation spectroscopyl, Analytical Chemistry 81 (2009) 465–472.
[29] T.J. Stasevich, F. Mueller, A. Michelman-Ribeiro, T. Rosales, J.R. Knutson, J.G. McNally, Cross-validating FRAP and FCS to quantify the impact of photobleaching on in vivo binding estimates, Biophysical Journal 99 (2010) 3093–3101.
[30] Y. Cheng, W.H. Prusoff, Relationship between the inhibition constant (K1) and the concentration of inhibitor which causes 50 per cent inhibition (I50) of an enzymatic reaction, Biochemical Pharmacology 22 (1973) 3099–3108.
[31] S. Chiantia, J. Ries, P. Schwille, Fluorescence correlation spectroscopy in membrane structure elucidation, Biochimica et Biophysica Acta 1788 (2009) 225–233.
[32] R. Das, S. Hammond, D. Holowka, B. Baird, Real-time cross-correlation image analysis of early events in IgE receptor signaling, Biophysical Journal 94 (2008) 4996–5008.
[33] D.A. Roess, S.M.L. Smith, P. Winter, J. Zhou, P. Dou, B. Baruah, A.M. Trujillo, N.E. Levinger, X. Yang, B.G. Barisas, D.C. Crans, Effects of vanadium-containing compounds on membrane lipids and on microdomains used in receptor-mediated signaling, Chemistry & Biodiversity 5 (2008) 1558–1570.
[34] Y. Chen, A.C. Munteanu, Y.-F. Huang, J. Phillips, Z. Zhu, M. Mavros, W. Tan, Mapping receptor density on live cells by using fluorescence correlation spectroscopy, Chemistry - A European Journal 15 (2009) 5327–5336.
[35] N. Andrews, K. Lidke, J. Pfeiffer, A. Burns, B. Wilson, J. Oliver, D. Lidke, Actin restricts FceRI diffusion and facilitates antigen-induced receptor immobilization, Nature Cell Biology 10 (2008) 955–963.
[36] N.L. Andrews, J.R. Pfeiffer, A.M. Martinez, D.M. Haaland, R.W. Davis, T. Kawakami, J.M. Oliver, B.S. Wilson, D.S. Lidke, Small, mobile FcεRI receptor aggregates are signaling competent, Immunity 31 (2009) 469–479.
[37] W.S. Hlavacek, A.S. Perelson, B. Sulzer, J. Bold, J. Paar, W. Gorman, R.G. Posner, Quantifying aggregation of IgE-FcεRI by multivalent antigen, Biophysical Journal 76 (1999) 2421–2431.
[38] R. Rigler, A. Pramanik, P. Jonasson, G. Kratz, O.T. Jansson, P.-Ã. Nygren, S. Stahl, K. Ekberg, B.-L. Johansson, S. Uhlen, M. Uhlen, H. Jörnvall, J. Wahren, Specific binding of proinsulin C-peptide to human cell membranes, Proceedings of the National Academy of Sciences of the United States of America 96 (1999) 13318–13323.
[39] L. Schäffer, A model for insulin binding to the insulin receptor, European Journal of Biochemistry 221 (1994) 1127–1132.
[40] L. Whittaker, C. Hao, W. Fu, J. Whittaker, High-affinity insulin binding: insulin interacts with two receptor ligand binding sites, Biochemistry 47 (2008) 12900–12909.
[41] C. Hao, L. Whittaker, J. Whittaker, Characterization of a second ligand binding site of the insulin receptor, Biochemical and Biophysical Research Communications 347 (2006) 334–339.
[42] Z.-H. Zhong, A. Pramanik, K. Ekberg, O.T. Jansson, H. Jörnvall, J. Wahren, R. Rigler, Insulin binding monitored by fluorescence correlation spectroscopy, Diabetologia 44 (2001) 1184–1188.
[43] K.H. Surinya, B.E. Forbes, F. Occhiodoro, G.W. Booker, G.L. Francis, K. Siddle, J.C. Wallace, L.J. Cosgrove, An investigation of the ligand binding properties and negative cooperativity of soluble insulin-like growth factor receptors, Journal of Biological Chemistry 283 (2008) 5355–5363.
[44] A. Chakravarty, J. Hinrichsen, L. Whittaker, J. Whittaker, Rescue of ligand binding of a mutant IGF-I receptor by complementation, Biochemical and Biophysical Research Communications 331 (2005) 74–77.
[45] A. Belfiore, F. Frasca, G. Pandini, L. Sciacca, R. Vigneri, Insulin receptor isoforms and insulin receptor/insulin-like growth factor receptor hybrids in physiology and disease, Endocrine Reviews 30 (2009) 586–623.
[46] S. Benyoucef, K.H. Surinya, D. Hadaschik, K. Siddle, Characterization of insulin/IGF hybrid receptors: contributions of the insulin receptor L2 and Fn1 domains and the alternatively spliced exon 11 sequence to ligand binding and receptor activation, Biochemical Journal 403 (2007) 603–613.
[47] G. Pandini, F. Frasca, R. Mineo, L. Sciacca, R. Vigneri, A. Belfiore, Insulin/Insulin-like growth factor 1 hybrid receptors have different biological characteristics depending on the insulin receptor isoform involved, Journal of Biological Chemistry 277 (2002) 39684–39695.
[48] M. Soos, C. Field, K. Siddle, Purified hybrid insulin/insulin-like growth factor-I receptors bind insulin-like growth factor-I, but not insulin, with high affinity, Biochemical Journal 290 (1993) 419–426.